Physica Scripta

PAPER

Nonlinear drift ion acoustic waves in degenerate plasmas with adiabatic trapping

IOP Publishing
Physica Scripta
Phys. Scr. 95 (2020) 045609 (6pp)
https://doi.org/10.1088/1402-4896/ab6e4b

Nonlinear drift ion acoustic waves in degenerate plasmas with adiabatic trapping

Amna Fayyaz[1], **H A Shah**[1], **M N S Qureshi**[1] **and W Masood**[2]

[1] Department of Physics, Government College University, Lahore 54000, Pakistan
[2] Department of Physics, COMSATS Institute of Information Technology (CIIT), Park Road, Islamabad Capital Territory, 45550, Pakistan

E-mail: hashah.gcl@gmail.com

Received 2 September 2019, revised 17 January 2020
Accepted for publication 21 January 2020
Published 19 February 2020

Abstract

In this work, we have investigated ion acoustic drift waves in the presence of adiabatically trapped degenerate electrons in both linear and nonlinear regimes. Using quantum magnetohydrodynamics (QMHD), we have modelled a new nonlinear wave equation with a fractional nonlinearity in two spatial dimensions and one temporal coordinate. We have carried out the nonlinear analysis by using Sagdeev potential approach and obtained arbitrary amplitude rarefactive solitons. The propagation ranges for these solitons are worked out with regard to inhomogeneity and obliqueness. For illustrative purposes, we have applied our results to neutron stars [5] where the quantum effects are surmised to be extremely significant.

Keywords: degenerate plasma, trapping, solitary wave, sagdeev potential

(Some figures may appear in colour only in the online journal)

1. Introduction

The pioneering theoretical framework to study quantum plasmas was laid down by Pines by including Pauli's exclusion term in the Boltzmann collision integral of Boltzmann–Vlasov model [1, 2]. Ever since, the interest in this field has grown manifold owing to its several applications in laser plasma interaction and nanoscale semiconductor devices which include quantum dots, quantum wells, carbon nanotubes and metal clusters [3, 4]. Quantum effects also play a crucial role in the dynamics of naturally occurring astrophysical plasmas in neutron stars and white dwarfs and this drawn significant attention of researchers in recent years [5]. As the dynamics of quantum mechanical systems are governed by the Fermi–Dirac statistics, the quantum hydrodynamic model (also quantum magnetohydrodynamic model) [6, 7] and transport models were developed by including the Bohm potential term whereas Wigner–Poisson model, which is the quantum analogue of classical Vlasov–Poisson model, was established by incorporating Pauli's exclusion term and spin effects [8, 9]. These models were further used to probe the dispersion properties of different wave modes in quantum mechanical arenas [10, 11]. Furthermore, nonlinear theory is well established in literature to study solitary structures in quantum plasmas, quantum vortices, wave-electron and wave–wave interactions. In [12], it was shown that ponderomotive force of an electromagnetic wave gives rise to magnetization and cyclotron motion in cold quantum plasmas which reduces with the increase in the frequency of the electromagnetic wave. Haas et. al investigated the quantum ion acoustic waves by employing the one-dimensional quantum hydrodynamic (QHD) model and derived the Korteweg–de Vries (KdV) equation for the weak nonlinear limit [13]. The travelling wave solutions of the nonlinear equation were also discussed which showed the nontrivial dependence on the Bohm Potential term and the wave mode was shown to reduce to its classical counterpart in the linear regime by ignoring the quantum effects. Similar treatment for electron acoustic waves [14] and nonlinear dust acoustic waves [15] was performed to obtain the KdV and modified KdV equations using the standard reductive perturbation technique to investigate the existence of compressive and rarefactive solitons and shock structures. The numerical analysis showed that width and amplitude of these structures had significant dependence on the quantum correction terms and the results were applied for the physical parameters that are typically found in ultra-dense astrophysical environments.

In 1957, Bernstein *et al* [16] studied the one-dimensional nonlinear stationary electrostatic wave in a collisionless plasma to demonstrate the effect of particles being trapped in the wave potential. These trapped particles undergo finite motion in the wave potential trough for which the travelling wave solutions of arbitrary form, amplitude and width can be obtained. This problem was extended to nonstationary adiabatic trapping by Gurevich using kinetic formulation in 1967 which yielded $3/2$ power nonlinearity instead of the usual quadratic nonlinearity [17]. The existence and properties of such stationary waves critically depend on the number of trapped particles which are supported by computer simulations and experimental investigations [18]. The trapping effect was also studied for the formation of vortices in classical plasmas by deriving the modified Hasegawa–Mima (HM) equation and analyzing the effect of bounce frequencies on the properties of trapped particles for both shallow and deep potential well cases [19, 20]. This work was followed by formulating the generalized HM for electron, positron and ion plasmas in order to investigate both the scalar and Jacobian nonlinearities incorporating the positron and electron temperature inhomogeneities. The addition of positrons was shown to lead to a broader class of solitary vortices [21]. Ion acoustic solitons were also studied using Maxwellian and non-Maxwellian distribution functions. The propagation properties were significantly modified particularly in the latter case where cusp solitons were obtained [22–24]. One of the significant investigations of trapping in quantum plasmas was done by Luque *et al* who studied the quantum corrected system of electron holes by solving Wigner–Poisson model using perturbation method [25]. Also, Demeio studied trapping effect for Bernstein–Greene–Kruskal equilibria in quantum phase space [26].

Shah *et al* found the expression for adiabatically trapped number density of electrons by virtue of an electrostatic scalar potential in the limits of partially and fully degenerate plasmas which we will use in our problem [27]. The effect of adiabatic trapping on the dispersion properties of ion acoustic waves in degenerate plasmas and relativistic degenerate plasmas in the presence of quantizing magnetic field were studied to obtain both compressive and rarefactive solitary solutions via Sagdeev potential approach and tangent hyperbolic (tanh) method [28–30]. Furthermore, drift solitary waves with trapped electrons have also been studied for the variation of electron degeneracy temperature in dense astrophysical plasmas [31]. Similarly, drift waves were investigated for electron–positron–ion (epi) plasmas with trapped electrons and positrons and derived KdV and Kadomtsev Petviashvili (KP) equations [32]. These equations were solved by tanh method and only compressive solitons were found. The characteristics of these compressive solitary solutions were found to have significant dependence on positron concentration, magnetic field and degeneracy temperature.

In our present work, we undertake the problem of nonlinear evolution of drift ion acoustic waves with the effect of trapped electrons in fully degenerate astrophysical plasmas. The dependence of the propagation characteristics of the solitary structures on number density, Mach numbers, obliqueness and inhomogeneity scale length are investigated. The arrangement of this manuscript is as follows. In section 2, we give the basic equations governing our problem. In section 3, we investigate the solitary structures by employing the Sagdeev potential technique. We discuss and summarize the results in section 4.

2. Mathematical formulation

We begin by considering a quantum magnetoplasma [7] consisting of ions and electrons with the ambient magnetic field $\boldsymbol{B_o}$ in the z-direction whereas density inhomogeneity is taken to be in x-direction i.e. $n_o(x)$. The wave phase velocity is considered to lie in the range $v_{\rm Fe} \gg \omega/k \gg v_{\rm Fi}$ ($v_{\rm Fe,Fi} = \hbar^2/m_{e,i}(3\pi^2 n_0)^{1/3}$ are the Fermi velocities of electrons and ions) and ions are taken to be cold and classical on account of their large mass by comparison with electrons i.e. $m_i \gg m_e$.

The momentum equation for ions is

$$m_i n_i(\partial_t + \boldsymbol{v_i}.\nabla)\boldsymbol{v_i} = en_i\left(\boldsymbol{E} + \frac{1}{c}\boldsymbol{v_i} \times \boldsymbol{B_o}\right) \tag{1}$$

here m_i, e and n_i are the mass, charge and number density of ions respectively. For the electrostatic wave, electric field takes the form $\boldsymbol{\mathcal{E}} = -\boldsymbol{\nabla}\varphi$, where φ is the scalar electrostatic potential. Assuming the usual drift wave approximation and the low wave frequency limit ($\Omega_{ci} \gg \partial_t$), the parallel and perpendicular components of ions velocity from equation (1) are given as follows

$$\hat{L}v_{iz} = -\frac{e}{m_i}\partial_z\varphi, \tag{2}$$

$$v_{i\perp} = \frac{c}{B_o}(\hat{z} \times \nabla\varphi) - \frac{c}{B_o\Omega_{ci}}\partial_t\nabla_\perp\varphi, \tag{3}$$

where the operator $\hat{L}$ is defined as $\hat{L} = \partial_t + \boldsymbol{v_E}.\nabla_\perp + v_{iz}\partial_z$ and $\Omega_{ci} = e\,B_o/\mathrm{c}m_i$ is the ion cyclotron frequency and $\boldsymbol{v_E} = \frac{c}{B_o}(\hat{z} \times \nabla\varphi)$ is the $\mathbf{E} \times \mathbf{B}$ drift. The number density for adiabatically trapped degenerate electrons in the presence of an electrostatic potential φ in degenerate plasma [27] is given as

$$n_e = n_o\{(1 + e\,\varphi/\varepsilon_F)^{3/2} + \pi^2T^2/8 \times\varepsilon_F^2(1 + e\,\varphi/\varepsilon_F)^{-1/2}\}, \tag{4}$$

where $\varepsilon_F = \hbar^2/2m_e(3\pi^2 n_0)^{2/3}$ is the Fermi energy, T is the temperature, k_B is the Boltzmann's constant and n_o is the background number density. It may be noted here that the second term on the RHS in equation (4) can be dropped for the fully degenerate plasmas as it is a small correction term for partially degenerate plasmas. The Poisson's equation is given by

$$\nabla^2\varphi = -4\pi e(n_i - n_e). \tag{5}$$

We substitute equation (4) for the fully degenerate case in equation (5) to get

$$n_i = -\frac{1}{4\pi e}\nabla^2\varphi + n_o\left(1 + \frac{e\varphi}{\varepsilon_F}\right)^{3/2}. \tag{6}$$

The continuity equation for ions reads as

$$\frac{\partial n_i}{\partial t} + \nabla.(n_i \boldsymbol{v}_i) = 0. \tag{7}$$

Substituting equations (2), (3) and (6) in equation (7) and collecting the terms under the condition $\partial_y > \partial_z > \partial_x$, we obtain the following equation for the coupled drift acoustic wave with fractional nonlinearity

$$\begin{aligned}&\partial_t^2(1+\Phi)^{3/2} - \lambda_{\mathrm{Fe}}^2\partial_t^2(\partial_y^2+\partial_z^2)(1+\Phi)\\ &- \rho_i^2\partial_t^2\partial_y^2(1+\Phi) + \frac{3}{2}v_*\partial_y\partial_t(1+\Phi)\\ &- c_s^2\partial_z^2(1+\Phi) = 0,\end{aligned} \tag{8}$$

where $\Phi = e\,\varphi/\varepsilon_F$ is the normalized electrostatic potential, $\lambda_{\mathrm{Fe}} = \sqrt{\varepsilon_F/4\pi e^2 n_0}$ is Fermi wavelength of electrons, $c_s = \sqrt{\varepsilon_F/m_i}$ is the quantum ion acoustic speed, $\rho_i = c_s/\Omega_{ci}$ is the ion Larmor radius and $v_* = (-2c\varepsilon_F/3eB_o)\kappa$ is the drift velocity in which $\kappa = |d_x \ln n_0|$ is the inverse scale length of density inhomogeneity. Equation (8) is a new ion acoustic drift wave equation with two spatial dimensions and one time coordinate that depicts the behavior of drift ion acoustic waves in fully degenerate plasma with the effect of adiabatically trapped electrons.

For the linear analysis of equation (8), we consider the sinusoidal perturbation which gives the linear dispersion relation for the coupled quantum drift ion acoustic wave (CDIAW) as follows

$$\omega = \frac{1}{2\gamma}\left[\omega_* \pm \left(\omega_*^2 + \frac{8}{3}c_s^2k_z^2\gamma\right)^{1/2}\right], \tag{9}$$

where $\gamma = 1 + 2/3\{(\lambda_{\mathrm{Fe}}^2 + \rho_i^2)k_y^2 + \lambda_{\mathrm{Fe}}^2k_z^2\}$, $\omega_* = v_*k_y$ is the drift frequency, $k_y = k\cos\theta$ $k_z = k\sin\theta$ are the wave numbers in the respective directions and θ is the angle between wavevector k and y-axis. Note that the factor $8/3$ comes from the expansion of the trapping term $(1+\Phi)^{3/2}$ in equation (8). This expression has no equivalent in classical plasmas as there the potential appears as $\Phi^{3/2}$ and, therefore, cannot be expanded [33]. The positive root of equation (9) is analyzed graphically in figure 1 by using the astrophysical plasma parameters such as those found in neutron stars [34] i.e. $n_o \sim 10^{26}$– 10^{29} cm^{-3}, $B_o \sim 10^9 - 10^{11}$ G, $c_s = 6\times10^7$ cm s^{-1}, $v_* = 5.9\times10^6$ cm s^{-1}, $\Omega_{ci} = 9.5\ \times 10^{14}$ s^{-1} and $\theta \sim \pi/18$ to $\frac{\pi}{6}$ which follows from the drift wave conditions ($k_y > k_z$ and $v_* \ll c_s$) [35]. The density regimes for the plasma are chosen so that the electrons remain nonrelativistic and degenerate. If the inhomogeneity is ignored (or $k_y \to 0$), equation (9) reduces into ion acoustic mode i.e. $\omega = \sqrt{2/3}\,c_s\,k_z\big/\sqrt{1 + 2/3\lambda_{\mathrm{Fe}}^2k_z^2}$ and drift wave [31] i.e. $\omega = \omega_*/1 + 2/3\{(\lambda_{\mathrm{Fe}}^2 + \rho_i^2)k_y^2\}$ for $k_z \to 0$ in fully degenerate plasmas. From figure 1, we observe that the frequency of the coupled drift ion acoustic wave increases as a function θ for the corresponding wavenumbers but for large values of k, there is no considerable variation in frequency.

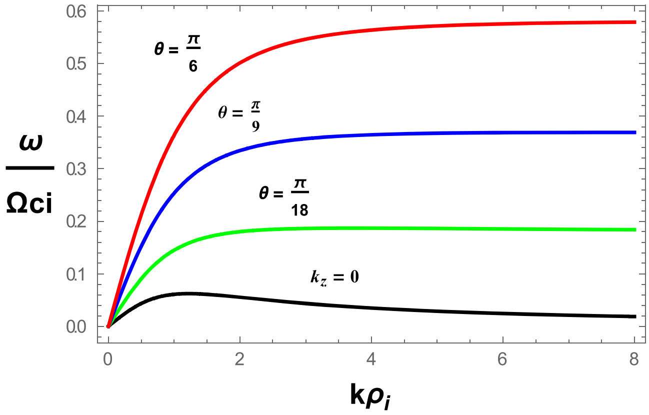

Figure 1. Linear dispersion relation of ion acoustic wave in inhomogeneous fully degenerate plasma for different values of θ ($n_o = 10^{27}$ cm^{-3} and $B_o = 10^{11}$ G).

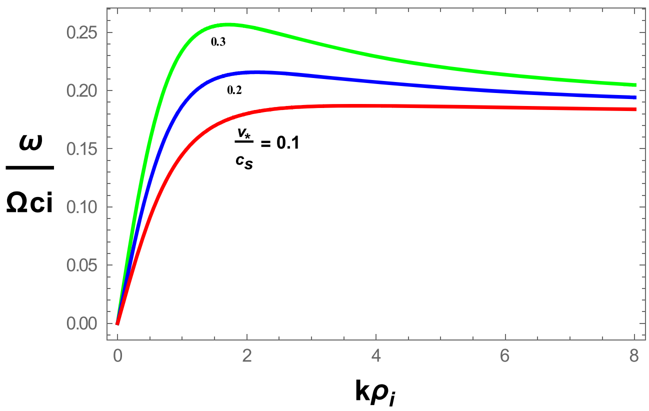

Figure 2. Linear dispersion relation with the variation in inhomogeneity for different values of $v_*/c_s(n_o = 10^{27}$ cm^{-3} and $B_o = 10^{11}$ G).

In addition to that, we have plotted $\omega(v_*)$ versus k in figure 2 at $\theta = \pi/18$ which shows that with the increase in v_* (or larger inhomogeneity κ), the frequency of the wave under consideration increases for the corresponding wavenumber in the linear pattern but for large k, the frequency becomes nearly constant.

3. New model equation with fractional nonlinearity

We now proceed to analyze equation (8) which is a new model nonlinear equation with fractional nonlinearity and use the Sagdeev potential approach for its nonlinear analysis. We transform equation (8) by using a co-moving frame $\xi = q_y y + q_z z - \Omega\,t$ where q_y and q_z are the nonlinear wave numbers and Ω is the nonlinear frequency of nonlinear structure. The transformed equation (8) reads as

$$\frac{\mathrm{d}}{\mathrm{d}\xi}\left\{\frac{\mathrm{d}}{\mathrm{d}\xi}(1+\Phi)^{3/2} - A\frac{\mathrm{d}^3}{\mathrm{d}\xi^3}(1+\Phi)\right\} - B\frac{\mathrm{d}^2}{\mathrm{d}\xi^2}(1+\Phi) = 0, \tag{10}$$

where $A = \{(\lambda_{\rm Fe}^2 + \rho_i^2)q_y^2 + \lambda_{\rm Fe}^2 q_z^2\}$ and $B = (c_s^2 q_z^2/\Omega^2 + 3\omega_*/2\Omega)$. Integrating twice using the boundary condition $\Phi \to 0$ as $\xi \to \infty$ for localized bounded solution yields

$$\frac{\mathrm{d}^2(1+\Phi)}{\mathrm{d}\xi^2} = \frac{1}{A}[(1+\Phi)^{3/2} - B\,(1+\Phi) - (1-B)], \tag{11}$$

where the last term in the parenthesis on the right-hand side of equation (11) is the constant of integration. It must be noted here that the term $(1+\Phi)^{3/2}$ which arises due to trapping effect in equation (8) is kept intact but in [36], this term had been expanded to obtain the solitary solutions by tanh method. Therefore, our selection of Sagdeev potential approach appears to be more pertinent and general for the analysis of equation (8). Introducing the Sagdeev potential by regarding the above expression as an energy law for a unit mass particle with position Φ oscillating in a potential well $W(\Phi)$ gives us the following expression

$$\frac{\mathrm{d}^2(1+\Phi)}{\mathrm{d}\xi^2} = -\frac{\mathrm{d}W(\Phi)}{\mathrm{d}\Phi}. \tag{12}$$

Equation (12) is integrated using the same boundary conditions mentioned above to evaluate the constants of integration which gives the Sagdeev potential $W(\Phi)$ as:

$$W(\Phi) = -\frac{2}{5A}(1+\Phi)^{5/2} + \frac{B}{2A}(1+\Phi)^2 + \frac{(1-B)}{A}(1+\Phi) - \frac{3}{5A} + \frac{B}{2A}. \tag{13}$$

Following the standard method given in [37, 38], the formation of solitary structures requires the following (i) that $\mathbf{W}(\boldsymbol{\Phi})_{\Phi=0} = 0$ and $\left(\frac{dW(\Phi)}{d\Phi}\right)_{\Phi=0} = 0$ so that an unstable fixed point obtains at the origin i.e. $(d^2\mathbf{W}/d\boldsymbol{\Phi}^2)_{\Phi=0} < 0$ and (ii) the function $\mathbf{W}(\boldsymbol{\Phi})$ must cross the $\boldsymbol{\Phi}$-axis for $\boldsymbol{\Phi} \lessgtr 0$; else it would imply an unbounded solution and no nonlinear structure would be formed. When $\mathbf{W}(\boldsymbol{\Phi}) < 0$ for $0 < \boldsymbol{\Phi} < \boldsymbol{\Phi}_{\rm max}$ it gives compressive solitons and when $\mathbf{W}(\boldsymbol{\Phi}) < 0$ for $\boldsymbol{\Phi}_{\rm min} < \boldsymbol{\Phi} < 0$ it gives rarefactive solitons where $\boldsymbol{\Phi}_{\rm max\,/\,min}$ is the maximum/minimum value of potential for $\mathbf{W}(\boldsymbol{\Phi}_{\rm max\,/\,min}) = 0$ i.e. the point where the curve cuts the positive/negative $\boldsymbol{\Phi}$ axis. The sign of the third derivative of equation (13) tells us whether the Sagdeev potential is positive potential structure or a negative potential structure [38]. In our case, the third derivative is negative so we will only get rarefactive structures. The range of propagation velocity $v = \Omega/q_y$ is given via Mach number which is defined as the ratio of velocity v to the quantum ion acoustic speed c_s. Now, expanding equation (13) and setting the quadratic term coefficient equal to zero, we obtain the following condition on the lower limit of Mach number $\mathcal{M}$ and is given as:

$$\mathcal{M}_l = \frac{1}{2}\left[\frac{v_* \cos\theta}{c_s} + \sqrt{\frac{v_*^2\cos^2\theta}{c_s^2} + \frac{8}{3}\sin^2\theta}\right], \tag{14}$$

where $\mathcal{M}_l$ is the lower Mach number. The condition on the upper Mach number $\mathcal{M}_h$ can be obtained by considering a physically valid solution, i.e. $\Phi_{\rm min} \leqslant -1$ and this gives

$$\mathcal{M}_h = \frac{5}{12}\left[\frac{3}{2}\frac{v_* \cos\theta}{c_s} + \sqrt{\frac{9}{4}\frac{v_*^2\cos^2\theta}{c_s^2} + \frac{24}{5}\sin^2\theta}\right]. \tag{15}$$

It is evident from equations (14) and (15) that the propagation range $\mathcal{M}_l < \mathcal{M} \leqslant \mathcal{M}_h$ depends on the drift velocity v_* and the propagation angle θ. Thus, these solutions yield a definite propagation range for a specific set of physical parameters. In figure 3, we present the Sagdeev potential plots $W(\Phi)$ versus Φ for $\theta = \pi/18$ for which the Mach number range is $0.19 < \mathcal{M} \leqslant 0.23$. These curves exhibit that the depth and the value of potential increase as the Mach number reaches its upper propagation limit. The corresponding rarefactive solitons $\Phi(\xi)$ versus ξ are given in figure 4 which show that for higher values of the Mach number $\mathcal{M}$, the amplitude of the solitary structure increases.

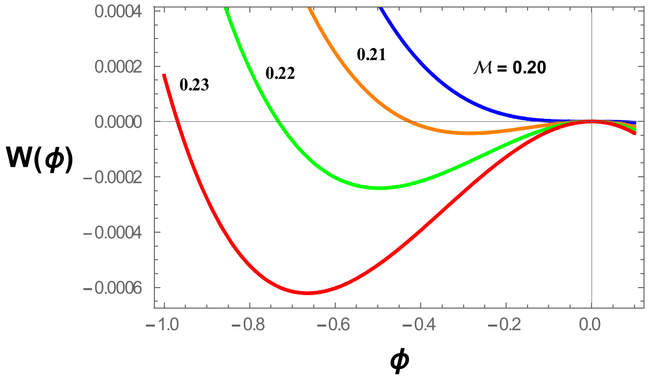

Figure 3. Plots for variation of Sagdeev potential $W(\Phi)$ versus Φ for different Mach numbers $\mathcal{M}$ at $\theta = \pi/18$ and $v_*/c_s = 0.1$.

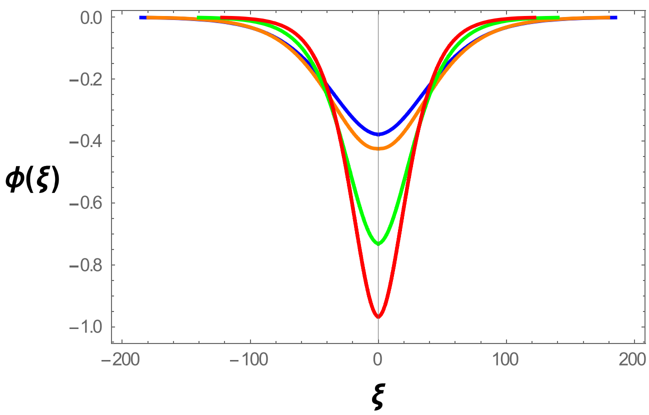

Figure 4. Rarefactive solitons for different Mach numbers $\mathcal{M}$ at $\theta = \pi/18$ and $v_*/c_s = 0.1$; $\mathcal{M}$ = (Blue, 0.20), (Orange, 0.21), (Green, 0.22), (Red, 0.23).

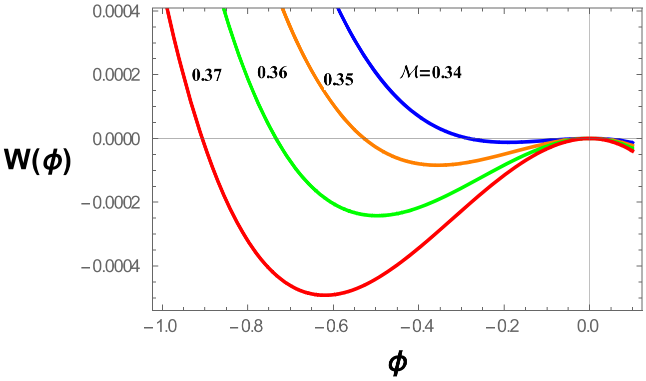

Figure 5. Plots for variation of Sagdeev potential $W(\Phi)$ versus Φ for different Mach numbers $\mathcal{M}$ at $\theta = \pi/9$ and $v_*/c_s = 0.1$.

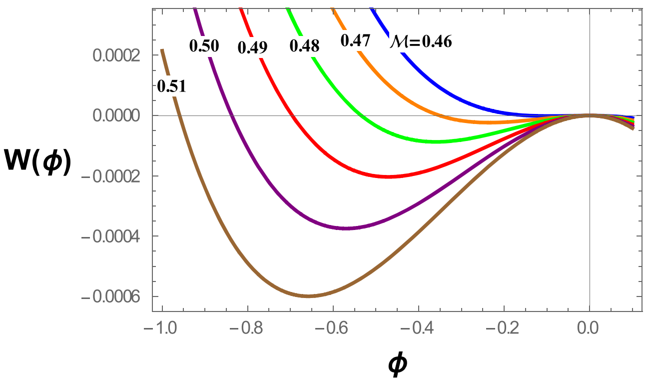

Figure 6. Plots for variation of Sagdeev potential $W(\Phi)$ versus Φ for different Mach numbers $\mathcal{M}$ at $\theta = \pi/6$ and $v_*/c_s = 0.1$.

Likewise, the Sagdeev potential curves for $\theta = \pi/9$ and $\theta = \pi/6$ are shown in figures 5 and 6 for which propagation regimes are found to be $0.33 < \mathcal{M} \leqslant 0.37$ and $0.45 < \mathcal{M} \leqslant 0.51$, respectively. These curves exhibit a similar increasing trend of variation in depth and potential as the Mach number reaches its maximum value for the respective case. It is also observed that the propagation regimes become a little broader with respect to $\mathcal{M}$ with the increase in obliqueness. On the other hand, for two slightly different angles with an identical Mach number (e.g. in figure 7 for $\theta = 0.12\pi$ and $\theta = 0.13\pi$, the identical Mach number is 0.40), the Sagdeev plots show that value of potential and the depth decreases drastically for a small increase in θ. These results are summed up in figure 8 where $\Phi_{\min}$ as a function of θ is plotted against the corresponding ranges of the Mach number. Furthermore, if we ignore the inhomogeneity κ or set $q_y \to 0$, the Mach number range becomes higher i.e. $0.81 < \mathcal{M} \leqslant 0.91$ and corresponds to (drift free) ion acoustic rarefactive solitons.

Another case pertinent to our problem arises from the variation in inverse scale length of inhomogeneity κ while keeping the other physical parameters constant. A slight variation in the inhomogeneity gives a unique propagation range for rarefactive solitons. The propagation regime when v_*/c_s is varied from 0.1 to 0.5 are depicted in figure 9 in which the change in $\Phi_{\min}$ can be seen as the Mach number slides from its lowest limit to upper limit for each case.

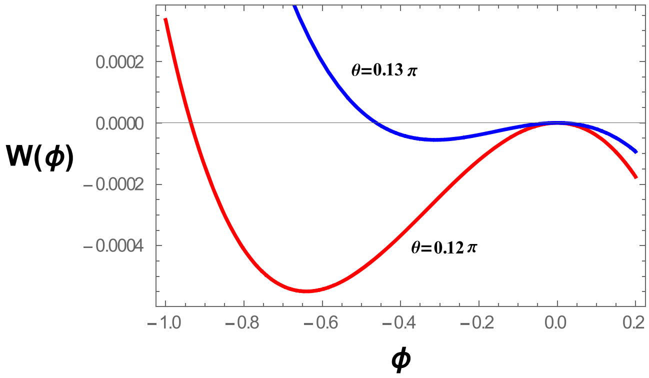

Figure 7. Plots for variation of Sagdeev potential $W(\Phi)$ versus Φ for Mach number $\mathcal{M} = 0.40$ at $\theta = 0.12\pi$ and 0.13π and $v_*/c_s = 0.1$.

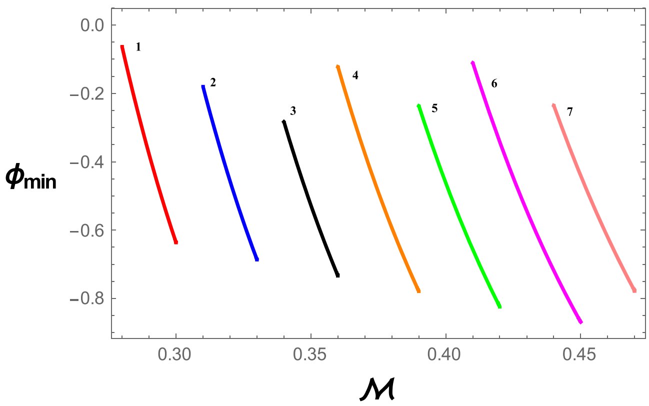

Figure 8. The amplitude of rarefactive solitons $\Phi_{\min}(\theta)$ versus Mach numbers $\mathcal{M}$ for $v_*/c_s = 0.1$; (1) $\theta = 0.08\pi$, (2)$\theta = 0.10\pi$, (3)$\theta = 0.12\pi$, (4)$\theta = 0.14\pi$, (5) $\theta = 0.16\pi$, (6) $\theta = 0.18\pi$, (7) $\theta = 0.20\pi$.

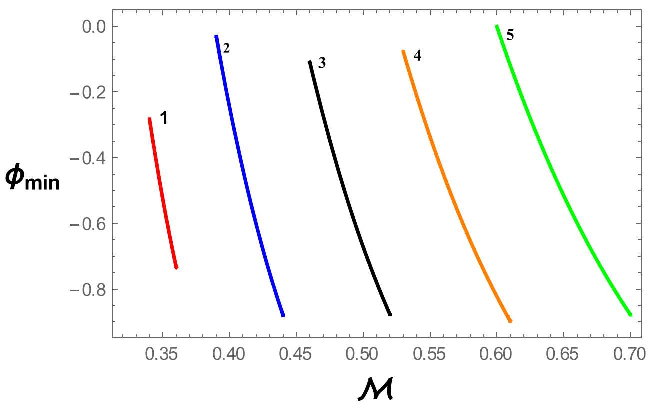

Figure 9. The amplitude of rarefactive solitons $\Phi_{\min}(v_*)$ versus Mach numbers $\mathcal{M}$ for $\theta = \pi/9$; (1)$v_*/c_s = 0.1$, (2) $v_*/c_s = 0.2$, (3) $v_*/c_s = 0.3$, (4) $v_*/c_s = 0.4$, (5) $v_*/c_s = 0.5$.

4. Summary and conclusion

We have investigated the propagation of quantum drift ion acoustic solitary waves in fully degenerate quantum plasmas. Using QMHD model, we have formulated a new nonlinear equation for the drift ion acoustic mode in the presence of trapped degenerate electrons bearing a fractional nonlinear term. This equation is analyzed in nonlinear regime by using Sagdeev potential approach to find the solitary structures. Further our model equation (equation 10) has been numerically investigated for neutron star plasma parameters and it is found that for these chosen parameters rarefactive solitary structures could exist. These solitary structures appear to have crucial dependence on angle of propagation and inhomogeneity. The nonlinear analysis presented here can be applied in a variety of physical situations of interest in astrophysical plasmas. It furthers our understanding of dealing with nonlinearities which appears as $(1 + \Phi)^{3/2}$ instead of classical trapping case where the nonlinearity appears as a $\Phi^{3/2}$ term. We hope to extend this work to investigating shock like structures in the dense astrophysical plasma environments.

Acknowledgments

This work has been supported by Higher Education Commission's research grant (8320/Punjab/NRPU/R&D/HEC/2017).

ORCID iDs

H A Shah https://orcid.org/0000-0003-1236-8825
M N S Qureshi https://orcid.org/0000-0003-3909-6305

References

[1] Pines D 1961 *J. Nucl. Energy* C **2** 5
[2] Wyld H W Jr and Pines D 1962 *Phys. Rev.* **127** 1851–5
[3] Loss D and DiVincenzo D P 1998 *Phys. Rev.* A **57** 120
[4] Kuo Y-H, Lee Y K, Ge Y, Ren S, Roth J E, Kamins T I, Miller D A B and Harris J S 2005 *Nature* **437** 1334–6
[5] Chabier G, Douchin F and Potekhin A Y 2002 *J. Phys.: Condens. Matter* **14** 9133
[6] Gardner C L and Ringhofer C 1996 *Phys. Rev.* E **53** 157
[7] Haas F 2005 *Phys. Plasmas* **12** 062117
[8] Manfredi G 2005 Fields Inst. Commun. (https://arxiv.org/pdf/quant-ph/0505004.pdf)
[9] Marklund M and Brodin G 2007 *Phys. Rev. Lett.* **98** 025001
[10] Manfredi G and Haas F 2001 *Phys. Rev.* B **64** 075316
[11] Shukla P K and Eliasson B 2007 *Phys. Rev. Lett.* **99** 096401
[12] Jung Y-D and Murakami I 2009 *Phys. Lett.* A **373** 969–71
[13] Haas F, Garcia L G, Goedert J and Manfredi G 2003 *Phys. Plasmas* **10** 3858–66
[14] Sah O P and Manta J 2009 *Phys. Plasmas* **16** 032304
[15] El-Labany S K, El-Siragy N M, El- Taibany W F and Behery E E 2009 *Phys. Plasmas* **16** 093701
[16] Bernstein I B, Green J M and Kruskal M D 1957 *Phys. Rev.* **108** 546
[17] Gurevich A V 1967 *Zh. Eksp. Teor. Fiz.* **53** 953–64
[18] Sagdeev R Z 1966 *Reviews of Plasma Physics* (4) ed M A Leontovich (New York: Consultants Bureau)
[19] Siddique H, Shah H A and Tsinsadze N L 2008 *J. Fusion Energy* **27** 216–24
[20] Arshad S, Shah H A and Qureshi M N S 2014 *Phys. Scr.* **89** 075602
[21] Kaladze T D, Shad M and Shah H A 2009 *Phys. Plasmas* **16** 024502
[22] Abbasi H, Tsinsadze N L and Tshakaya D D 1999 *Phys. Plasmas* **6** 2373
[23] Chuang S H and Hau L N 2009 *Phys. Plasmas* **16** 022901
[24] Mushtaq A and Shah H A 2006 *Phys. Plasmas* **13** 012303
[25] Luque A, Schamel H and Fedele R 2004 *Phys. Lett.* A **324** 185–92
[26] Demeio L 2007 *Transp. Theory Stat. Phys.* **36** 137–58
[27] Shah H A, Qureshi M N S and Tsinsadze N 2010 *Phys. Plasmas* **17** 032312
[28] Masood W, Karim S, Shah H A and Siddiq M 2009 *Phys. Plasmas* **16** 112302
[29] Shah H A, Masood W, Qureshi M N S and Tsinsadze N L 2011 *Phys. Plasmas* **18** 102306
[30] Iqbal M J, Masood W, Shah H A and Tsinsadze N L 2017 *Phys. Plasmas* **24** 014503
[31] Shah H A, Masood W, Asim M T and Qureshi M N S 2014 *Astrophys. Space Sci.* **350** 615–22
[32] Shaukat M I 2019 *Indian J. Phys.* **93** 683–90
[33] Lifshitz E M and Pitaevskii L P 1981 *Physical Kinetics* (*Course of theoretical Physics* 10) (Oxford: Permagon Press plc)
[34] Chabrier G, Douchin F and Potekhin A Y 2002 *J. Phys.: Condens. Matter* **14** 9133–9
[35] Weiland J 2000 *Collective Modes in Inhomogeneous Plasma* (Bristol and Philadelphia: Institute of Physics Publishing) 0
[36] Shaukat M I 2017 *Eur. Phys. J. Plus* **132** 210
[37] Chen F F 1984 *Introduction to Plasma Physics and Controlled Fusion* 1 ed 2 (New York: Plenum Press) 0-306-41332-9
[38] Mamun A A 1997 *Phys. Rev.* E **55** 1852